Quantitative Trait Loci Affecting Components of Wing Shape in *Drosophila melanogaster*

Erika Zimmerman, Arnar Palsson and Greg Gibson

Department of Genetics, North Carolina State University, Raleigh, North Carolina 27695-7614

Manuscript received September 27, 1999
Accepted for publication February 10, 2000

ABSTRACT

Two composite multiple regression-interval mapping analyses were performed to identify candidate quantitative trait loci (QTL) affecting components of wing shape in *Drosophila melanogaster* defined by eight relative warp-based measures. A recombinant inbred line design was used to map QTL for the shape of two intervein regions in the anterior compartment of the wing, using a high resolution map of retrotransposon insertion sites between Oregon-R and Russian 2b. A total of 35 QTL representing up to 23 different loci were identified, many of which are located near components of the epidermal growth factor-Ras signal transduction pathway that regulates vein *vs.* intervein decision making and vein placement. Over one-half of the loci were detected in both sexes, and just under one-half were detected at two different growth temperatures. Different loci were found to affect aspects of shape in each intervein region, confirming that the shape of the whole wing should be regarded as a compound trait composed of several developmental units. In addition, a reciprocal backcross design was used to map QTL affecting shape in the posterior compartment of the wings of 831 flies, using a molecular map of 16 allele-specific oligohybridization single nucleotide polymorphism (SNP) markers between two divergent inbred lines. A total of 13 QTL were detected and shown to have generally additive effects on separable components of shape, in both sexes. By contrast, 8 QTL that affected wing size in these backcrosses were nearly dominant in their effects. The results confirm at the genetic level that wing shape is regulated independent of wing size and set up the hypothesis that wing shape is regulated in part through the regulation of the length and positioning of wing veins, involving quantitative regulation of the activity of secreted growth factors.

ORGAN and appendage development can be divided into two phases: the generation of positional information across a field of cells and refinement of mature sizes and shapes. Molecular genetic dissection of wing development in Drosophila has delineated how the dorsal-ventral and anterior-posterior axes of the wing are established and how secreted morphogens emanating from these organizing regions set up the locations of the future wing veins, thereby providing a general description of pattern formation in the wing (see de Celis 1998; Morata and Sanchez-Herrero 1999; Strigini and Cohen 1999 for reviews). Genetic dissection of the refinement phase may also follow from the analysis of individual mutations, but since shape is a quantitative phenotype it can also be studied using the methodologies of quantitative genetics. An understanding of the genetic basis for variation in the degree of roundness or pointedness of wings, their breadth and narrowness, or in the asymmetric placement of particular veins will require identification of polymorphisms that affect these traits. The first step toward this end is the identification of quantitative trait loci (QTL).

Corresponding author: Greg Gibson, Department of Genetics, Gardner Hall, North Carolina State University, Raleigh, NC 27695-7614. E-mail: ggibson@unity.ncsu.edu

The principle of recombination mapping is that loci that affect a trait can be localized by virtue of their association with genetic markers that differ between two parental strains and can be readily traced in progeny generations. This approach was initially proposed by Sax (1923) using visible markers, but in recent years it has been adopted using anonymous molecular markers such as microsatellites, restriction fragment length polymorphisms, and single nucleotide polymorphisms (SNPs). In interval mapping, estimates of the association between genotype and phenotype are made throughout the genome by using recombination probabilities between each pair of markers to estimate the likely genotype at each position between the markers (Lander and Botstein 1989). The statistical power and accuracy of interval mapping can be increased further by the process of composite multiple regression-interval mapping (CIM; Zeng 1993), in which the estimates of genotype-phenotype associations are conditioned on marginal associations elsewhere in the genome. While CIM does not have the resolution to support the positional cloning of new genes, it does support the mapping of QTL at a resolution of a few centimorgans, depending on marker density (Zeng 1994). In Drosophila, this resolution combined with the existing detailed genetic map generally allows the identification of candidate genes that may be responsible for the QTL effects (Mackay 1996).

Wing shape presents an alternative model system to bristle number (Mackay 1996) for quantitative genetic dissection in Drosophila. The shape of each intervein region (IVR) in wild-type flies is regulated independently of the shape of the other intervein regions (Birdsall *et al.* 2000). This observation is consistent with molecular genetic data that indicate that wing veins are positioned according to cellular responses to the secreted morphogens Decapentaplegic, Wingless, and Hedgehog (Strigini and Cohen 1999). Moreover, the shapes of intervein regions are remarkably constant across temperature and sex, despite the fact that female wings are uniformly 15% larger than male wings, as are the wings of flies raised at 18° rather than at 25° (see de Moed *et al.* 1997; James *et al.* 1997 for recent discussions of reaction norms for wing size in Drosophila). Since cell number and cell size are affected by sex and temperature differently in particular regions of the wing, we have argued that shape is defined by a mechanism that is independent of cell growth and density and proposed that the lengths of the wing veins may be critical in establishing genotype-specific wing shapes (Birdsall *et al.* 2000). This hypothesis then establishes genes involved in vein-intervein determination and differentiation as candidate genes for QTL affecting wing shape.

In this article we report the results of two different QTL mapping experiments that confirm that different genes contribute to variation in each intervein region of the wing. The first experiment involved a set of 96 recombinant inbred lines that derive from 2 isogenic parental lines (Oregon-R and Russian 2b) that have statistically indistinguishable overall wing shapes. The similarity is deceptive, though, since it is actually a result of complementary variation in anterior and central intervein regions. These lines had been genotyped previously according to the position of 94 roo transposons on polytene chromosome squashes, which afforded the possibility of high resolution QTL mapping (Nuzhdin *et al.* 1997). The second experiment involved two isogenic lines (W6 and W29) that were chosen for this study on the basis of morphological divergence in the posterior compartment of their wings. Approximately 200 individuals of each sex in backcrosses between F_1 progeny and each parental type were genotyped at 16 SNPs using the allele-specific oligohybridization (ASO; Saiki *et al.* 1986) method, providing low resolution mapping with the opportunity to document the dominance of QTL effects. QTL profiles in the experiments were not greatly affected by sex or growth temperature and suggest the involvement of known regulatory genes in the refinement of wing shape.

MATERIALS AND METHODS

Flies: The set of 96 recombinant inbred (RI) lines derived from the cross of Oregon-R by Russian 2b were provided by Drs. Jeff Leips and Trudy Mackay at NCSU and have been described previously (Nuzhdin *et al.* 1997). They were raised on standard cornmeal medium supplemented with live yeast. In most cases, larval density was controlled by transferring 30 first instar larvae from a collection plate to a single vial. The two 25° replicates were grown 3 months apart, but the two 18° replicates were grown concurrently.

Lines W6 and W29 (Gibson and van Helden 1997) were chosen from a preliminary survey of wing shape in a dozen isofemale lines (Birdsall *et al.* 2000). Near-isogenic lines were generated by 15 generations of sib-pair inbreeding, at which point each of the 16 molecular markers were scored to confirm that the parents were homozygous at each marker. The F_1 generation was set up with two pairs of W6 male and W29 virgin females, and each of the backcrosses (BC) were performed between 15 single virgin F_1 females and a male of the respective parental line. Between 10 and 15 2- to 3-day-old adults of each sex were taken from each vial, for a total of 211 BC-W6 females, 212 BC-W6 males, 203 BC-W29 females, and 205 BC-W29 males. The crosses were performed at 25°.

Markers: The genetic map for the RI lines was based on the previously published set of retrotransposon insertion sites in the lines, modified slightly by the removal of several adjacent markers that did not show any recombination (J. Leips and T. F. C. Mackay, unpublished results). This left a set of 81 independent markers, including the Sparkle visible marker on chromosome 4 (which did not show any significant QTL associations and is not considered further here). There is a single gap in the map on chromosome arm 2R, between markers 50F and 57C, which were separated by >50 cM as a consequence of map expansion in recombinant inbred lines. QTL located within the gap would be missed in our analysis. The terminal markers were at 1B, 19C, 21E, 60E, 61A, and 100A, which in all cases are very close to the telomeres (or centromere of the X).

PCR primers and ASO sequences for each of the 16 markers used to map the BC populations are shown in Table 1. Each of the four combinations of backcross and sex yielded very similar maps, so these were combined to generate a common map file for the QTL mapping. This enabled direct comparison of QTL locations across experiments in Figure 4, but may have slightly distorted the precise location of QTL peaks. The agreement between our genetic map and the published crossover frequencies for the 16 markers was excellent, with the exception of the *DopR* marker. *DopR* was initially mapped to 35EF by an unpublished polytene hybridization squash (Gotzes *et al.* 1994), but genetically maps to the vicinity of cytological bands 88–89. The cDNA sequence is identical to sequence within BACR03J06, which maps to 88B, so we conclude that the position defined by our recombination frequencies is correct.

ASO genotyping (Saiki *et al.* 1986) was performed as follows. A total of 20 μl of PCR products generated with Taq DNA polymerase were blotted directly from 96-well microtiter plates onto nylon filters (Hybond N^+; Pharmacia Biotech, Piscataway, NJ) under vacuum and fixed by UV irradiation. ^{32}P end-labeled 15-mer allele-specific oligonucleotides were hybridized to the filters in 10 ml of hybridization solution, and stringency washes were performed in 5× SSPE, 0.1% SDS at the temperatures indicated in Table 1. Hybridization was detected by autoradiography after between 2 and 8 hr of exposure according to the age of the probe. Both the perfect match and mismatch probes were hybridized to all filters, providing a control for success of the PCR reactions. Fewer than 5% of the genotypes for 16 markers across 831 individuals (584/13,296) were represented as missing data.

Morphometrics: Wings were dissected from both sides of the body, simply mounted in rows on a microscope slide, and

TABLE 1

PCR and ASO oligonucleotide sequences

Name	PCR primer sequence	Name	ASO sequence	Temp.[a]
AC-LMPX1	TTGCAGGACCGAATGGATCG	ACaso1	gtgttgatgagctgg	53
AC-RMPX1	CTCGAATCCAAAGTCGTAGG	ACaso2	ccagctcgtcaacac	55
SEV-LMPX1	CCACTCCAGTTACCAGATCA	SEVaso1	tggacacgaactcaa	47
SEV-RMPX1	CTTGGAGAAGGAGAACGACT	SEVaso2	ttgagtttgtgtcca	46
FOG-LMPX1	CCTTCGGGAGAGGCCAGTAA	FOGaso1	cccggcgtcgatttg	57
FOG-RMPX1	TGTGGAGAAGGCATCACTGG	FOGaso2	cggcggcgtcgattt	55
NIN-LMPX1	ACAACAAGAAGCCGGTGGGC	NINaso1	gactgttcgggaagc	49
NIN-RMPX1	GGAAGTTGGCCACCGTCTTG	NINaso2	gctttccgaagagtc	49
DMTKV-F	GTTGAATGCGCAGTTCCGACC	TKVaso1	tgtaacatacattaa	RT
DMTKV-R	TGCTCTTACAGGCTAGTCATC	TKVaso2	ttaaagtatgctaca	RT
DMAPT-F	CTTGGACTAACGGATGCTCAG	APTaso1	acacgtttaacgccc	52
DMAPT-R	GCTTGGTAAAAACATTGCCAGC	APTaso2	gggcgtttaacgtgt	52
EVE-LMPX1	GTTTGCTGGGATTAGCCAAG	EVEaso1	ccaatcctgatccct	50
EVE-RMPX1	ATTGGGATTGGGATCGGGCT	EVEaso2	agggatcgggattgg	52
DMTR2-F	GTGTGCAATATAGCAGGGAATC	TR2aso1	ccggacataaggacc	43
DMTR2-R	TTCGTTCGCGATCGCGTGATC	TR2aso2	ggtccttgtgtccgg	43
DPT-LMPX1	TTATCCGATGCCCGACGACA	DPTaso1	tgaagcccactccac	52
DPT-RMPX1	CCGCCTCCCTGAAGATTGAG	DPTaso2	gtggagttggcttca	51
R-LMPX1	GACCTGCGCGAGCAGATACT	Raso1	aggacacagacgatg	50
R-RMPX1	GTCGCACTTGTTGCCCACGA	Raso2	catcgtccgtgtcct	54
DMTPH-F	CAGTGGAGAAACCCGAGAATC	TPHaso1	gcgcatatattggaa	RT
DMTPH-R	CCTCGACTATGTAAGCCGAATC	TPHaso2	gcatataaaatgtact	RT
DMFZ-F	GTGCTCACCTTCTTGATTGAC	FZaso1	atattctcagcatga	43
DMFZ-R	GGATTTCCACAGAACTTACCTTC	FZaso2	attcgttcacagcat	45
Ras1-AF	GCTAAGAAACGGTGATGCCAG	RASaso1	ccgtctgcctgtgtg	56
Ras1-AR	GACTGTGCGTGTATGGGCTGC	RASaso2	cacacagccacacgg	RT
DMDOP-F	CCGTATCACGTATCCGACCAC	DOPaso1	aggagtttcgcgacg	51
DMDOP-R	GCAAGTGACATGTGTCACTCC	DOPaso2	cgtcgcggaactcct	57
DMS-LMPX1	CAAGGAGCGCAACATGTGGT	DMSaso3	gcgaatcctgcgtgt	52
DMS-RMPX1	CCTCTGATTGGCTGACGGCA	DMSaso4	tttgtgcgtgtatat	47
DMTLL-F	CCTCACAGCAGACAACACAAC	TLLaso2	aagacacaccagtgc	55
DMTLL-R	GGCATTCTCGGACTCGTAGAC	TLLaso1	cgcaataccgccgtc	50

[a] Temp., wash temperature.

then flattened with a cover slip held in place with a piece of tape. Low magnification images were captured as TIFF files in Adobe Photoshop using a SPOT camera mounted on a Nikon Eclipse E-800 microscope attached to a Dell Dimension 350 computer and stored digitally on compact discs for later measurement. Area and length ratios were calculated as described in Birdsall *et al.* (2000) directly with Scion Image software [a PC version of NIH Image (Rasband 1995), downloaded from http://www.scioncorp.com]. Landmark coordinates at the junctions of longitudinal veins with the wing margin or crossveins were also captured with this program and then transferred to a Microsoft Excel worksheet.

Relative warps were calculated with the TPSRelw program of Rohlf (1993) downloaded from http://www.stonybrook.edu/morphometrics. This program first transforms shapes defined by the landmark coordinates into generalized least squares Procrustes shapes by reducing them to unit area and rotating them to an optimal alignment. It then computes the principal warps for the tangential configuration of the total data set (1 for IVR-B and IVR-D; 2 for IVR-C), the partial warps that describe the vectors that transform each individual shape from the consensus shape, and finally the relative warps. Relative warps can be thought of as principal components of the local shape transformations, namely of the positions of the landmarks (Bookstein 1991, 1994).

We also performed QTL analyses directly on principal components of the correlation matrix of the Procrustes landmark coordinates (Dryden and Madia 1998) using JMP Version 3 (SAS Institute 1995) and on ratio measures specific to each compartment. Principal component analysis yielded almost identical results for the first and second relative warps but slightly divergent results for the third ones. The correlation between the values of the first two measures for each individual in each experiment was >0.95 and >0.6 for the third measure. Note that several of the QTL identified for the third warp were not seen with the corresponding principal component measure.

For the results presented in the figures and tables, relative warps were calculated on three separate data sets: the 25° and 18° replicates of the RI lines and the combined W6 $\times$ W29 backcrosses. Line means for each sex (for the RI sets) were calculated as least squares means using PROC GLM in SAS (SAS Institute 1990) and individual means (for the BC set) were calculated directly in Microsoft Excel, from the relative warp scores for each individual wing. All analyses were repeated using relative warp scores calculated from the reduced data sets for each sex or backcross separately (data not shown). This had no marked effect on the shape of the QTL profiles, providing added confidence in the robustness of the statistical measure.

QTL analysis: QTL were identified using model 6 in QTL Cartographer Windows Version 1.01 (Basten *et al.* 1999) downloaded from http://statgen.ncsu.edu/qtlcart/, with either 5 or 10 background parameters (chosen by forward stepwise regression) and a 10-cM window size. As shown in Table 3, the number of background parameters affects the likelihood ratios, as well as the estimates of additive effects. In general, the lower number of background parameters leaves more significant peaks, while the higher number increases the likelihood ratios of the most significant peaks. We present both in the interest of a balance between conservatism and reducing the false negative detection rate. Significance thresholds were determined by 100 random permutations of each relative warp data set, with 1% and 5% values set by the highest, and highest five, peak likelihood ratios. A likelihood ratio >3.86 corresponds to a 0.05 alpha value for each marker considered alone, but the permutation thresholds are needed to confront the problem that multiple comparisons are performed (see Zeng 1994 for a discussion of statistical thresholds in composite multiple regression-interval mapping).

Since several of the QTL exceed the threshold for only one of the background parameters, these should be regarded as marginally significant, but it should also be noted that many of them are associated with peaks in both sexes and temperatures, which increases confidence that they correspond to true QTL. To test whether individual QTL were sex or environment specific, two-way ANOVA was performed with the genotype (G) of the nearest marker, the sex (S) or temperature (E), and the $G \times S$ or $G \times E$ interactions as dependent variables. For the RI line experiment, the genotypes of markers nearest each significant QTL for the particular trait were included as covariates. For the BC experiment, a similar procedure was used to test for dominance, by assigning BC6 homozygotes and BC29 heterozygotes as class A, BC6 heterozygotes and BC29 homozygotes as class B, and testing the $G \times Class$ interaction.

RESULTS

Wing shape variation in two sets of crosses: The outline shapes of the wings of Oregon-R and Russian 2b flies are very similar, but differences in vein location lead to differences in shape of the IVRs defined by the second and third (IVR-B) and third and fourth (IVR-C) wing veins. In Oregon-R flies, IVR-C is relatively narrow and IVR-B is relatively broad, whereas the opposite situation pertains to Russian 2b flies. This difference is not simply due to a shift in placement of the third vein, or accommodation of increased breadth of one IVR by loss of breadth of the other (Guerra *et al.* 1997), because recombinant inbred lines derived from a cross between the two lines can be narrow or broad in both IVRs, as shown in Figure 1, A and B. The shape of each of these IVRs must then be regulated independently of one another. The number of rows of cells across each IVR is significantly, but only weakly, correlated with the length-to-breadth ratio ($R^2 < 0.2$; $P < 0.001$, ANOVA), indicating that IVR shape is a function of more than just the number of cells between veins. To begin to characterize the genetic architecture of these shape differences, we have conducted a QTL analysis of the shape of both wings in five flies of two replicates of each sex, at both 18° and 25°, for 96 recombinant inbred lines.

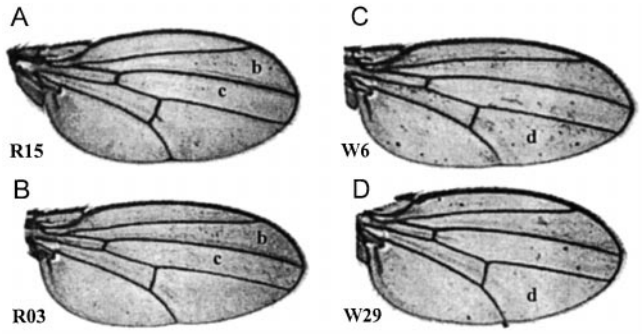

Figure 1.—Range of variation in wing morphology. Images of male right wings with anterior up and distal to the right. (A and B) Two RI lines that show greater than average breadth (A, R15) or narrowness (B, R03) in both intervein regions in the anterior compartment. (C and D) Similar differences in overall wing shape can arise from variation restricted to IVR-D in the posterior compartment, as typified by lines W6 (C) and W29 (D). Female wings are 15% larger, but show essentially the same shape differences. b, IVR-B; c, IVR-C; d, IVR-D.

By contrast, the outline shapes of W6 (a line from Capetown, South Africa) and W29 (a Kenyan line) are significantly different, in large part due to the difference in breadth of IVR-D, which is distal to the posterior crossvein and defined by the fourth and fifth longitudinal veins, as shown in Figure 1, C and D. IVR-B and IVR-C do not have significantly different shapes in these two lines. To identify QTL affecting the shape of IVR-D, we have scored wing shape in slightly more than 200 flies of each sex, grown at both 25° and 18°, in both backcross directions, that is, between F_1 females and W6 or W29 males. We also present an analysis of wing size, which is not correlated with wing shape in this cross.

Shape can be measured in a number of ways, including the geometric morphometric technique of relative warp analysis (Bookstein 1991). Relative warps capture the principal components of local shape transformations, and are a strictly relative measure since they are calculated by reference to the consensus shape (or "tangent configuration") for the entire data set under consideration. Despite the high degree of algebraic manipulation, the resultant measures capture much more of the between-line variation than do more intuitive measures, such as length-to-breadth ratios, and have the advantages of distinguishing different aspects of shape and not being biased by preconceptions.

The effects of each relative warp can be seen visually by plotting consensus coordinates of the flies with the highest and lowest values for each relative warp (Figure 2). For IVR-C in the recombinant inbred lines, relative warp 1 (hereafter C1) captures some of the breadth of the intervein region, but is most strongly affected by the position of the posterior crossvein. C2 is highly correlated with the length-to-breadth ratio (data not shown) and is a good measure of compartment width, while C3 captures shape variation near the wing margin. For

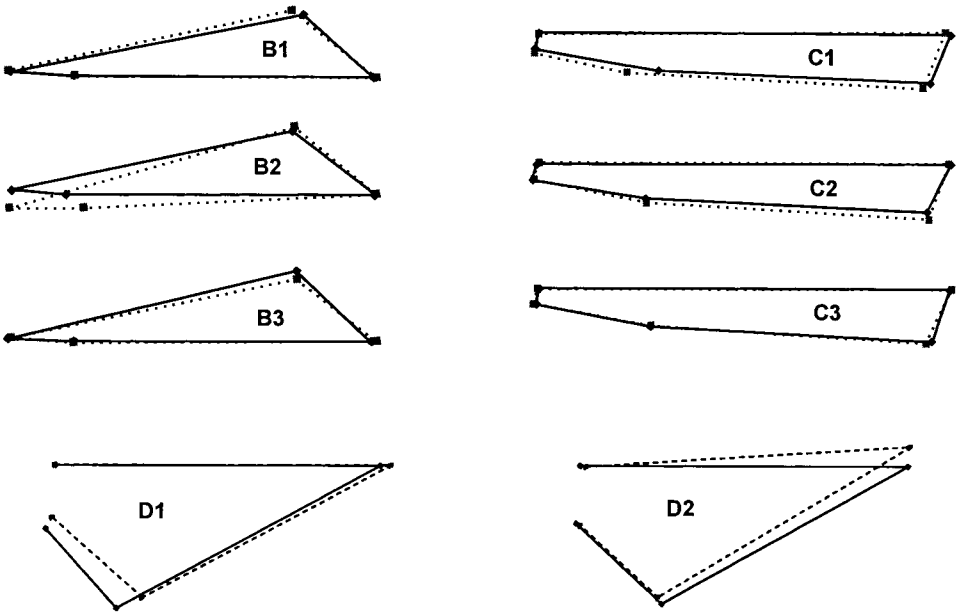

Figure 2.—Shape variation captured by relative warps. The consensus Procrustes coordinates of the five RI lines (or individuals for IVR-D) with the most extreme values of each of the indicated relative warps that account for 90% of the shape variation (B1–B3; C1–C3; D1 and D2) are aligned and plotted to show the most likely parameters of the transformations captured by each warp. B1 and B3 affect the location of the junction of longitudinal veins 1 and 2, while B2 may capture more proximal variation. C1 is heavily affected by the location of the posterior crossvein, C2 most closely captures the length-to-breadth ratio of IVR-C, while C3 has a subtle effect on the distance between longitudinal veins 3 and 4 at the wing margin. D1 appears to affect the length and placement of the posterior crossvein and distal portion of longitudinal vein 5, while D2 is related to the length of the distal longitudinal vein 4 and its placement at the wing margin. Despite the marked differences in shape of IVR-D, the number of cells along the wing margin in this region was not significantly different in this cross (data not shown).

IVR-B, B1 and B3 are related to breadth while B2 appears to be strongly influenced by the location of the anterior crossvein. For IVR-D in the W6 by W29 backcrosses, only two relative warps are considered, and while there are a variety of ways to align the consensus shapes, it appears that D1 captures the relative length and location of the distal portion of longitudinal vein 5, while D2 captures shape variation closer to the wing margin.

Summary statistics for each cross are presented in Table 2. Sex does have a significant effect on each of the relative warps, which causes the means to deviate from zero, but these effects are small relative to between-line differences, as seen by the range of scores. When relative warps are determined independently by sex or temperature, the absolute values differ markedly, but the correlation between values is extremely high, and as a result QTL profiles are almost identical. This indicates that the relative warp measures are remarkably robust within a cross. In all cases the relative warp scores were normally distributed, although there were three lines with higher than expected values of C1 and B2. Within-line variance was typically just twice the between-side variance within an individual, and these two sources of error accounted for between 20 and 30% of the total phenotypic variance. The two parents in each cross were separated by between four and six standard deviation units for each relative warp score. In the following analysis, QTL effects were estimated in standard deviation units on the basis of the least-squares line means (or individual means, for IVR-D).

QTL analysis of shape in the anterior compartment of the wing: QTL affecting wing shape were identified using the CIM algorithm implemented by model 6 in QTL Cartographer (Zeng 1994; Basten *et al.* 1999). Throughout, effect estimates were obtained at 1-cM intervals, with background markers chosen at a minimum spacing of 10 cM. Since peak locations and heights determined by CIM are sensitive to the number of background markers used to condition estimates within each interval, results are presented in Table 3 for both 5 and 10 background markers. Experiment-wide 5% and 1% likelihood ratio thresholds were determined by permutation analysis and had values of 9–11 and 13–17, depending on which warp and sex was considered. Consequently, QTL peaks are listed only if they exceed a likelihood ratio of 15 in either conditioning background (5 or 10 background markers), or 10 with both conditions.

For the anterior compartment of the wing, recombinant inbred line means for each sex and temperature were calculated from 20 wings, namely the left and right sides of five individuals of each of two replicate vials. QTL profiles with 10 conditioning markers are shown in Figure 3 for two representative relative warps, B1 and C2, with 18° females shown by bold lines, 25° females by regular lines, 18° males by hairlines, and 25° males by dotted lines. The three chromosomes are represented from left to right, corresponding to cytological map positions from 1 to 100, and marker locations are indicated by a short vertical line beneath each plot. Peaks are numbered according to their listing in Table 3.

A total of 35 QTL were identified, corresponding to 23 separate loci as a result of the observation that 9 of the QTL were associated with two or more of the six

TABLE 2

Summary statistics for relative warp scores

	25°					18°					25°			
	B1	B2	B3	C1	C2	C3	B1	B2	B3	C1	C2	C3	D1/6	D1/29	D2/6	D2/29
♀ Mean	6.06	1.87	3.51	1.15	4.19	2.11	5.21	4.05	2.29	0.88	3.74	0.82	13.6	0.9	6.3	1.2
♀ SD	0.89	0.93	0.47	1.20	0.47	0.35	12.13	7.92	5.60	17.88	5.60	3.50	14.7	12.7	9.7	7.7
♀ Range	40.5	52.9	23.9	71.8	21.3	16.6	69.5	42.8	25.7	108.2	29.6	18.2	70.7	74.9	56.0	49.6
♂ Mean	−6.47	−1.71	−3.32	−1.80	−4.19	−2.03	−5.50	−3.99	−2.29	−1.39	−3.63	−0.69	15.1	−11.4	−1.3	−6.3
♂ SD	0.86	0.84	0.58	1.16	0.48	0.35	11.39	7.61	6.38	17.48	5.53	3.47	14.9	13.7	9.0	7.0
♂ Range	40.3	47.6	25.7	79.0	19.7	16.7	69.7	38.9	30.1	106.2	31.8	18.5	75.8	76.8	44.9	36.9
% Variance	50.8	29.9	16.1	60.5	19.6	10.3	52.1	28.5	16.2	70.9	14.7	6.8	68.6		16.0	

D1/6 and D1/29 are values associated with D1 for BC6 and BC29, respectively. The sign of each warp is arbitrary, so these have been adjusted for IVR-B and IVR-C to make the mean values positive for females and negative for males. Ranges and standard deviations (SD) are among line means for IVR-B and IVR-C, and among individuals for IVR-D. All values are 1000 times the actual values reported by TPSRelw.

relative warps studied. Just over one-half of the QTL (20/35) were present in both sexes, and just under one-half of them (15/35) were present at both temperatures. These fractions should be considered as underestimates since several QTL were associated with peaks that exceeded the marker-wise, but not experimentwise, significance threshold in sex and temperature combinations other than those listed in Table 3 and so are likely to be false negatives. A total of 13 QTL were found in just one sex and temperature combination, while 4 were common to all four combinations.

These results establish that a common suite of genes is responsible for much of the variation in wing shape, independent of variables that affect wing size, such as sex and growth temperature. Examples of apparently male-specific (B1.4), female-specific (B1.2, B1.3, and C1.3), and 18°-specific (B1.4, B2.7, and C2.4) QTL suggest that sex- and temperature-specific genetic factors may exist, underlining the genetic complexity of the trait. However, two-way ANOVA failed to confirm the statistical significance of these specificities, so that a more critical interpretation is that QTL analysis in crosses derived from parents that are separated by just a few environmental standard deviation units has low power to repeatedly detect specific QTL. This view is consistent with the presence of a further eight loci that were present in three of the four analyses.

Each intervein region, and each relative warp within a region, appears in the main to be regulated by different genes, as expected from the low genetic correlation between shapes of intervein regions and the fact that each warp captures a slightly different aspect of shape (see also Birdsall *et al.* 2000). However, six loci at similar genetic locations were identified in both IVRs, which may reflect the fact that IVR-B and IVR-C are both bounded by the third longitudinal vein. Effects with opposite signs, indicating that the increasing allele derived from different parents, were found for five of the relative warps, the exception being the third warp of IVR-B. Only three QTL were found for C1 (compared with between five and seven for the other warps) even though it accounted for more than half of the shape variance for IVR-C. This may be attributed to the high variance in the placement of the anterior crossvein relative to the other landmarks and suggests that this aspect of shape is affected by a few alleles with stronger effects than those that account for variation elsewhere in the wing. Average QTL effects ranged from 0.2 to 0.8 standard deviation units of the particular relative warp. The proportion of the variance explained for each relative warp ranged from 10 to 70%, but there is no obvious way to express the proportion of the overall shape variation explained by individual QTL.

QTL analysis of shape in the posterior compartment of the wing: For IVR-D in the posterior compartment of the wing, we measured the relative warps of just over 200 individuals of each sex in both backcross directions from the cross of W6 and W29 flies and tested these

TABLE 3

QTL identified in recombinant inbred lines

				Female 25°			Male 25°			Female 18°			Male 18°		
QTL	Location	Interval	Candidates	LR10	LR5	Effect[Sig.]	LR10	LR5	Effect[Sig.]	LR10	LR5	Effect[Sig.]	LR10	LR5	Effect[Sig.]
								IVR-B							
B1.1	3.314–3.320	99A	wings down	13.1	17.7	−0.40**	26.7	26.4	−0.74***	11.6	11.6	−0.40*			
B1.2	1.114–1.116	13B	Turneduplike	17.6	14.4	0.69**	13.4	3.1	0.77[m.s.]						
B1.3	3.059–3.060	65CD	vvl/Cf1a	14.5	5.5	−0.45*	16.6	5.5	−0.51*						
B1.4	3.173–3.174	85F	Ras1; blistery				11.9	8.1	−0.43*				15.5	5.9	−0.41*
B1.5	2.084	29F	?							16.9	10.1	0.36*	11.1	6.3	0.34[m.s.]
B1.6	1.090	10BC	dishevelled				12.5	9.5	0.50*						
B1.7	3.197	88F	punt				12.4	6.5	0.33*						
B2.1	2.161–2.167	46DE	tapered				53.9	34.7	−0.77***	23.5	22.3	0.48***	26.0	18.1	0.50**
B2.2	3.004–3.005	61CD	emc				14.6	17.0	0.41**	13.3	11.5	0.35*	13.8	1.6	0.25[m.s.]
B2.3	3.035	62A	veinlet	15.2	5.9	0.48*									
B2.4	3.148	72A	argos				8.9	18.1	0.33*						
B2.5	2.084	29F	?	7.3	12.9	−0.23*									
B2.6	3.182–3.186	87EF	messy	5.4	12.6	0.21*				20.9	20.8	0.42**	20.8	14.4	0.41**
B2.7	3.069–3.060	62C	veinlet							11.7	7.8	−0.24[m.s.]	14.1	6.7	−0.29[m.s.]
B3.1	3.104–3.106	68AB	crossveinless-3	36.1	25.1	0.48***	22.4	15.1	0.42**	31.1	21.6	0.50***	22.5	23.3	0.44***
B3.2	2.154–2.165	47CF	schnurri	9.3	15.6	0.35*	13.1	16.0	0.32**	16.3	22.8	0.50**			
B3.3	2b.002–2b.010	57EF	EGFR	16.2	10.1	0.35**	12.0	7.8	0.25*				14.1	12.6	0.41*
B3.4	3.063	65BC	divergent	33.3	22.5	0.65***							29.3	26.0	0.48***
B3.5	2.122–2.124	33AE	spalt	14.8	7.5	0.39*							18.5	31.6	0.45**
B3.6	3.319	99A	wings down							3.5	16.7	0.36*	11.0	13.1	0.25*
B3.7	3.343	100A	warts				17.3	11.1	0.28**						
								IVR-C							
C1.1	2.159	46BD	tapered				18.2	16.0	0.57**						
C1.2	2.181	50CD	drk				16.5	16.0	−0.58**						
C1.3	3.315–3.323	99A	wings down	14.0	10.6	−0.43*				7.6	10.6	−0.32[m.s.]			
C2.1	3.150–3.155	73AD	argos	34.7	32.6	−0.48***	19.6	44.5	−0.40***	27.4	29.2	−0.45***	17.6	12.9	−0.45**
C2.2	2.181	50CD	drk				15.3	8.7	0.34*	15.6	12.5	0.45**	14.1	12.6	0.44*
C2.3	1.033	4F	?				14.4	4.2	0.28[m.s.]	11.5	15.1	0.46*	17.5	16.3	0.47**
C2.4	2.141–2.144	37	spitz							12.2	9.2	0.30*	20.3	7.7	0.33*
C2.5	3.060	65CD	vvl/Cf1a	18.2	11.5	−0.46**									
C3.1	2.181	50CD	drk; short stop	27.1	17.6	−0.64**	21.1	13.6	−0.50**	29.5	23.6	−0.63***	39.3	30.3	−0.77***
C3.2	3.319–3.321	99A	wings down	11.4	15.0	0.29*	3.0	29.0	0.26*	15.7	12.5	0.31*	15.5	24.0	−0.37**
C3.3	3.164	77E	knirps				12.8	18.4	0.44**						
C3.4	3.195	88D	punt							29.7	12.3	−0.40**			
C3.5	1.096	10D	dishevelled							16.4	13.3	0.74*			
C3.6	3.248	94CD	hedgehog							19.2	8.1	0.31*			

QTL are named for the IVR (B or C) and number of the relative warp (1, 2, or 3). LR10 and LR5 refer to likelihood ratios with 10 and 5 background parameters, respectively. Genetic map positions were defined by Kosambi mapping function in QTL Cartographer. Cytological positions were inferred relative to locations of flanking retrotransposon markers. Candidate genes are loci within QTL intervals that have a known wing phenotype. Effects are expressed as standard deviation units for the line means of the RI lines for each trait. Significance values are: [m.s.] marginal; * LR $<$ 15 for one set of background parameters; ** threshold $<$ LR $<$ 20 for both parameters; *** LR $>$ 20 for both parameters.

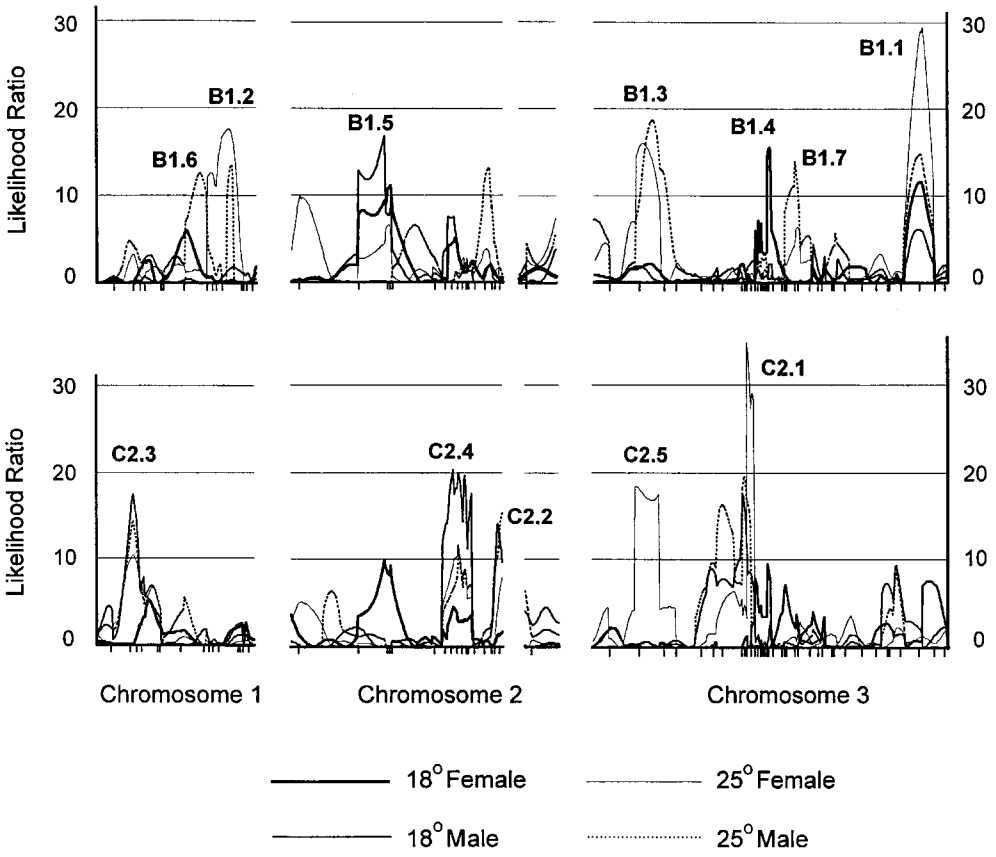

Figure 3.—QTL profiles for relative warps in the anterior wing. Likelihood ratios (LR) are plotted against chromosomal location for relative warps B1 (top) and C2 (bottom), using results from the analysis with 10 background parameters. The value of the LR at each position in the genome reflects the probability of an association between the genotype at that position and the phenotype. Peaks in the profile represent locations of putative QTL. The experimentwise LR significance threshold for B1 at 25° was 11.2, and for C2 was 10.5. B1.5 and C2.5 may actually represent two QTL, but by convention are regarded as single peaks since the troughs in the likelihood distribution do not drop below the significance threshold.

against the locations of 16 molecular markers. Relative warps D1 and D2 explained, respectively, 68 and 16% of the total shape variance and were associated with six and five QTL peaks as plotted in Figure 4 and summarized in Table 4. Particularly for D1, this is likely to be an underestimate of the number of QTL, as the effect of the QTL centered near the centromere on chromosome arm 2L (D1.2) was so large that it may be due to several

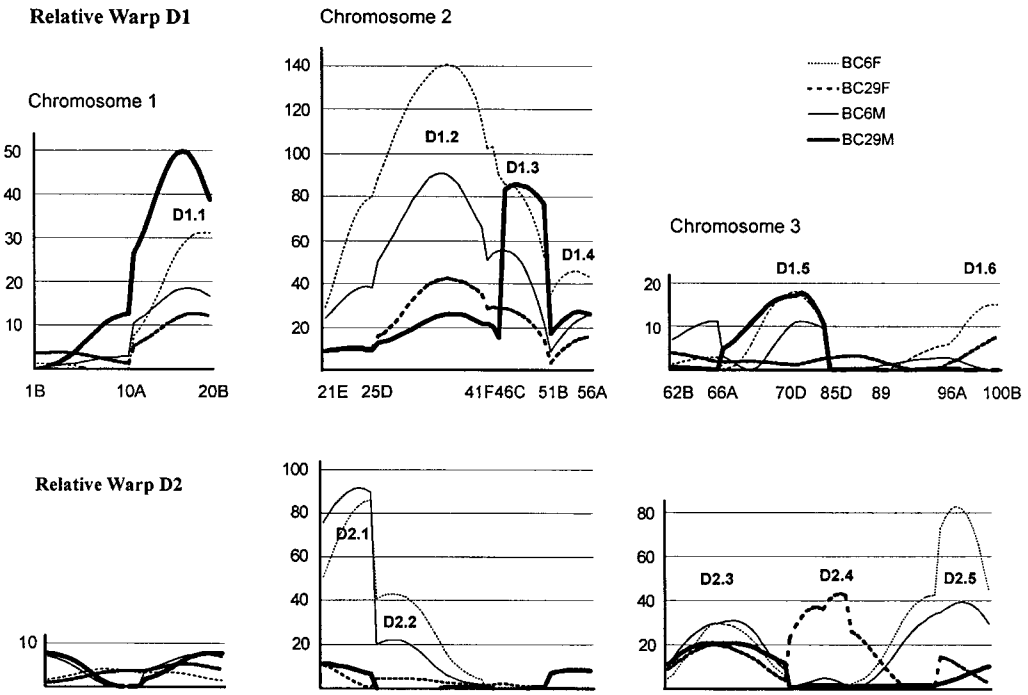

Figure 4.—QTL profiles for relative warps in the posterior wing. Likelihood ratios plotted against chromosomal location for relative warps D1 (top) and D2 (bottom), using results from analysis with five background parameters. Locations of the 16 ASO markers are indicated between the two profiles. QTL peak positions in Table 4 were estimated using the Kosambi mapping function. Thick lines, BC29; solid lines, males. Experimentwise LR thresholds were 12.5 and 11.2 for D1 and D2, respectively. All peaks indicated are highly significant.

TABLE 4

Wing shape QTL identified in W6 × W29 backcrosses

QTL	Location	Interval	Type (P)[a]	♀ BC6	♀ BC29	♂ BC6	♂ BC29	Candidates
D1.1[b]	1.053	14–17	Additive	0.50	−0.46	0.48	−0.94	*small wing* (PLC-γ); *Beadex*
D1.2[b]	2.041	31–32	Part. dom. (<0.01)	1.36	−1.03	1.36	−0.82	*abrupt*; *Proxless*; *salm*
D1.3[b]	2.066	46–48	Additive	1.04	−0.85	0.95	−1.13	*engrailed*; *tapered*
D1.4	2.082	54–55	Additive	0.67	−0.57	0.60	−0.69	*narrow*
D1.5	3.043	70–80	Complex (<0.02)	0.35	—	0.34	−0.47	
D1.6	3.108	99–100	♀ dom. (<0.0001)	0.32	—	—	—	*Medea*
WR.1	1.014	5–6	♂ specific	—	—	0.26	−0.48	*curlex*; *crossveinless*
D2.1[b]	2.012	24–25	Dominant (<0.001)	1.03	—	1.12	—	*fat*
D2.2	2.024	27–28	Dominant (<0.001)	0.95	—	0.86	—	*wingless*
D2.3	3.024	66–68	Additive	0.60	−0.64	0.70	−0.63	*hairy*
WR.6	3.030	68–70	Complex	0.30	−0.72	—	−0.64	*Gap1*
D2.4	3.059	87–90	♀ dom. (<0.001)	—	−0.96	—	—	*punt*
WR.7	3.085	95–96	Additive	−0.78	0.61	−0.30	0.40	
D2.5	3.101	98–99	Complex (<0.001)	−1.08	0.51	−0.73	—	*wings down*

Estimates of additive effects in standard deviation units for the cross and sex.
[a] Numbers in parentheses refer to level of significance of inference regarding dominance (see text).
[b] Also detected as WR QTL.

linked loci. The large span of these QTL compared to those identified for the anterior compartment is due to the much larger separation between ASO markers (average 20 cM) compared with retrotransposon insertion sites (average 3 cM). The extremely high likelihood ratios associated with the majority of the peaks can be attributed to the increased number of individuals compared with the recombinant inbred line experiment. It also attests to the low environmental noise associated with relative warp measures.

QTL were also detected for a more direct measure of shape, the length-to-breadth ratio of the entire wing. Four of the seven peaks identified with this measure corresponded to relative warp QTL. This confirms that much of the shape difference between W6 and W29 wings is confined to IVR-D. The remaining three wing ratio (WR) QTL may indicate factors that regulate aspects of posterior wing shape not captured by relative warps, or they may be due to variation elsewhere in the wing.

Performance of a double backcross experiment allowed us to estimate the dominance of QTL effects, simply by contrasting the estimates of the effects in each cross. Only 2 of the 13 different QTL for shapes appeared to be completely dominant, while the remainder were essentially additive, or showed some partial dominance. The correspondence between the sexes was remarkably high for this analysis. Only D1.1, D2.4, and D2.5 were confirmed to be sex specific by significance of the genotype-by-sex interaction term in ANOVA of the nearest-marker genotype ($P = 0.02$, 0.005, and 0.03, respectively), although 3 other QTL showed some trend toward sex specificity in the degree of dominance. Dominance effects were confirmed by combining the two backcrosses and treating the experiment as an artificial F_2 design, and then testing the significance of nonadditivity in QTL Cartographer (data not shown), as well as by testing interaction terms of nearest markers by two-way ANOVA as indicated in Table 4. In all but two cases the IVR-D QTL had effects in the direction predicted from the differences between the parental lines.

The additivity of wing shape effects is in marked contrast to the dominance of each of eight QTL for overall wing size detected in the same W6 by W29 backcross experiment. Two of these size QTL had large effects exceeding one standard deviation unit. Positive and negative effects were found in both parents, which is not surprising since the two lines were not preselected for size differences. Only one size QTL was specific for a single sex (WS5 in females, $P = 0.03$), which is consistent with the fact that the magnitude of the difference in size between the sexes is fairly constant across lines. This result also contrasts with the sex specificity of more of the shape effects and reinforces the conclusion that size and shape are regulated by different suites of genes. Candidate genes within the QTL intervals are indicated in Table 5, and notably include the genes *wingless*, *fat*, *small wing*, *messy*, and *Hairless*, all of which have been found by mutational analysis to affect aspects of cell growth and division.

DISCUSSION

Meaning of QTL peaks: Two different strategies have been used to map QTL affecting components of wing shape in the anterior and posterior compartments of the wing. These have resulted in profiles with different resolution and significance levels, but nevertheless identify several highly significant QTL for each intervein region. The two major advantages of using recombinant inbred lines are that each genotype is represented by

TABLE 5

Wing size QTL identified in W6 × W29 backcrosses

QTL	Location	Interval	Type[a]	♀ BC6	♀ BC29	♂ BC6	♂ BC29	Candidate genes
WS1	1.018	6–7	Additive (n.s.)	0.32	−0.67	0.46	−0.65	
WS2	1.048	12–13	Part. dom. (<0.03)	—	−0.95	0.44	−0.84	*small wing* (PLC-γ)
WS3	2.012	23–24	Dominant (<0.001)	−1.73	—	−1.47	—	*fat*
WS4	2.024	27–28	Dominant (<0.001)	−1.81	—	−1.57	—	*wingless*
WS5	2.077	52–53	♀ spec. dom. (<0.001)	—	−0.69	—	—	*curved*; *Upturned*
WS6	3.034	67–70	Dominant (<0.01)	−0.66	—	−0.53	—	*crossveinless-3*
WS7	3.054	87–88	Dominant (<0.04)	—	−0.51	—	−0.47	*messy*
WS8	3.070	92–93	Dominant ? (n.s.)	0.56	—	0.51	—	*Hairless*

Estimates of additive effects in standard deviations units for the cross and sex.
[a] Numbers in parentheses refer to level of significance of inference regarding dominance (see text).

multiple individuals, which leads to reduction in the environmental component of variance, and that it has allowed the generation of a high density genetic map (Nuzhdin *et al.* 1997), with the result that most QTL peaks are localized to <2 cM, and usually a single cytological band. The Oregon-R and Russian 2b lines were not preselected for any differences in wing shape, and in fact the wing shape differences between them by no means cover the range of variation seen in even the anterior intervein regions in *Drosophila melanogaster*, yet the RI lines allowed efficient detection of QTL.

The W6 and W29 lines by contrast were chosen on the basis of divergent wing shapes following inbreeding, and this divergence turned out to be restricted to IVR-D. Our analysis demonstrates the feasibility of mapping QTL between any two wild-type lines of interest. The advantages of the backcross design are that it allows estimation of dominance effects and takes less than a month to perform the crosses once the near-isogenic parental lines have been constructed. In principle, between 20 and 40 PCR products can be obtained from the genomic DNA of a single fly, allowing a low to moderate resolution QTL map to be generated with just a few months of marker genotyping. Microsatellite (Schug *et al.* 1998) and single nucleotide polymorphism (Teeter *et al.* 1999; http://www4.ncsu.edu/~ggibson) marker collections have been described that will allow rapid QTL mapping with F_2, backcross, or recombinant inbred line designs. Although the peaks identified with this method may only be mapped to within two or three cytological intervals, and linked QTL may often go unresolved, the availability of the complete genome sequence will allow higher resolution mapping. SNPs are sufficiently frequent that they can be identified with efficiency by sequencing 500-bp PCR products from the parental lines (Teeter *et al.* 2000), allowing a second phase of mapping, if necessary, with a fresh set of individuals.

Relative warp and principal component analysis of landmark coordinates are highly efficient methods for characterizing components of shape. Compared with other trait measures such as length-to-breadth ratios, the geometric morphometric measures increase the number and significance of QTL peaks identified. They also break shape variation down into components that appear to capture biologically reasonable shape vectors, such as the location of a crossvein, or breadth near the wing margin. However, there is no strong reason to expect that they actually capture vectors of underlying gene effects, which operate over unknown distances within the developing imaginal discs. Consequently, the relative warps are likely only to be correlated with aspects of shape variation that could be detected if we could precisely know the cell biological mechanisms underlying variation in wing morphology. This in turn implies that the observed QTL probably underestimate the number and magnitude of QTL effects for the wing traits. Several peaks at or close to the significance threshold appear in the analysis, but there is no way of knowing whether these would attain significance with a perfect way to characterize wing shape.

The major drawback of relative warps is that the measures cannot be contrasted directly between two different crosses. This is true of any measure that captures the difference between individuals and a standard shape that is specific to each cross. In principle, different crosses could be contrasted if the standard shape was set in advance, perhaps as the grand mean for the species (note that this is not true of direct principal component analysis of landmark coordinates). However, it is likely that any QTL that also have a significant effect in a second cross will also be identified in that cross, even though they may be associated with different relative warps. If the goal of the QTL analysis is to identify the loci that have a significant effect on the trait, the logical strategy is to use the statistically most powerful procedure to locate the QTL and then follow up with functional studies of the mechanism by which they affect the trait (Liu *et al.* 1996), once candidate genes in the region have been identified. Several of the QTL described here lie in the vicinity of peaks identified by Weber *et al.* (1999) in their dissection of the third chro-

mosome contribution to wing shape using a very different trait measure, but no statistical comparison of our results has been attempted.

Candidate genes for QTL affecting wing shape: In this study we have identified over a dozen strong QTL affecting various aspects of wing shape and have evidence for up to a dozen other loci with less strong effects. In general, different loci affect the shapes of each intervein region, and these loci can act for the most part in both sexes and independent of the effect of temperature. Within a species, crosses between just two lines will not generally segregate all of the quantitative trait loci affecting any given trait (Mackay 1996). Some QTL may be due to rare alleles that by chance are present in the parental lines, but there is no way to address this question without considerably more population sampling. The results suggest, in agreement with those of Weber *et al.* (1999), that up to 50 loci throughout the genome may have a significant and generally additive effect on wing shape in *D. melanogaster*. This would place one candidate gene every two or three cytological intervals, which is about one-half of the density of genes known from Mendelian phenotypes to affect wing shape.

Nevertheless, the locations of QTL peaks listed in Tables 3 and 4 provide some hints as to the nature of the developmental pathways that contribute to variation in shapes of the intervein regions. Most notably, 6 of the 21 putative candidate genes for IVR-B and IVR-C are located in the same cytological band as components of the epidermal growth factor (EGF)-Ras signaling pathway that regulates vein *vs.* intervein cell determination (reviewed in Freeman 1998; Nagaraj *et al.* 1999). These are the *EGFR*, the ligands encoded by *spitz* and *argos* (Simcox 1997), the cofactor *rhomboid*/*veinlet* (Guichard *et al.* 1999), and two components of the intracellular signal transduction cascade, *Ras1* and *drk* (Simon *et al.* 1993). Four other genes, *spalt*, *emc*, *messy*, and *ventral veinless*, interact genetically with this pathway and may represent target genes. Two genes, *schnurri* and *punt*, are components of the Decapentaplegic morphogen signaling pathway that initially defines where the longitudinal veins will form. Furthermore, the region of 62A to 65F that includes *emc*, *veinlet*, *vvl*, and *divergent* showed a complex set of peaks that were unresolved in some analyses (see peak C2.5 in Figure 3) and may also include the EGF receptor (EGFR) ligand *vein* and the intracellular regulator of signal transduction, *sprouty*, as candidate genes. *A priori*, the Wingless, Hedgehog, and Notch signaling pathways might have been expected to be implicated in the regulation of wing shape, but there is no strong evidence implicating these pattern formation mechanisms (see Flybase for extensive references).

A test for the significance of association with a set of candidate genes has been proposed by Keightley *et al.* (1998), who summed the LOD scores of four genes implicated in obesity in mice and compared this number with those derived from a sample of permutations of four random markers in the same experiment. We modified this test for multiple traits by summing the number of times the marker closest to each candidate gene exceeded the experiment-wide 5% significance threshold for each warp of IVR-B and IVR-C in both sexes of the 25° recombinant inbred experiment. One trouble with this test is that *a priori* clustering of candidate genes is somewhat arbitrary. Nevertheless, each of the groups (*EGFR*, *vn*, *argos*, and *ve*: 4 loci, 7 peaks), (*EGFR*, *vn*, *argos*, *ve*, *dpp*, *tkv*, *put*, *sax*, and *shn*: 9 loci, 12 peaks), and (*EGFR*, *vn*, *argos*, *ve*, *bs*, *dpp*, *tkv*, *put*, *sax*, *shn*, *en*, *wg*, *apt*, and *vg*: 14 loci, 16 peaks) fall within the top 3% of 50,000 random permutations of sets of an equal number of markers spaced at 10-cM intervals on the RI map. These tests provide some support for associations between wing shape and, respectively, the EGF receptor-ligand complex, the EGF and transforming growth factor-β receptor-ligand combinations, and a general set of wing patterning genes.

Overall wing shape is correlated with the breadth of the distal proximal region of the wing (Birdsall *et al.* 2000), so it is interesting that several of the QTL for IVR-D are located in the vicinity of candidate genes whose names indicate a general role in wing shape: *fat*, *narrow*, *tapered*, *Proxless*, *abrupt*, and *small wing*. The roles of most of these genes in wing development have yet to be characterized in any detail, and several of them have yet to be cloned, so it is not possible to say whether they may operate in a common pathway. *Engrailed*, *spalt*, and *wingless* are particularly interesting candidates given their fundamental roles in wing patterning, but their involvement would be more strongly supported if other genes with which they interact were also implicated as QTL.

Only a few QTL in the W6 by W29 cross appear to be associated with wing size as well as wing shape, consistent with the low phenotypic correlation between these traits. Given the low resolution of the molecular map, it is impossible to say at this point whether the common QTL peaks are due to the same candidate genes, such as *small wing* and *wingless*. One argument against them being the same is the observation that most of the factors affecting wing shape only show partial dominance, or additivity, while those affecting wing size are essentially dominant. This remarkable feature of the genetic architecture may relate to the roles of directional and balancing selection in shaping the genetic variation of different aspects of wing morphology, or to a difference in the frequency of rare recessives affecting size *vs.* shape. A more interesting possibility is that the degree of dominance is a function of the underlying physiology of gene activity affecting the two processes (Kacser and Burns 1981; Mayo and Burger 1997). Identification of the genes that are actually responsible for the QTL effects will be the necessary next step in the quantitative genetic dissection of wing shape.

Utility of QTL mapping in Drosophila: Despite the obvious advantages of flies for quantitative genetic mapping, only two morphological traits have been analyzed previously by interval mapping methods: bristle number (Mackay 1996) and male genital morphology (Liu *et al.* 1996). Progress with the respect to the latter has been limited by the paucity of information on the genetics of development of the genital disc, but the wealth of information on neurogenesis in Drosophila has led to profound advances in our understanding of quantitative aspects of bristle development. Building on QTL associations, Mackay, Langley, and co-workers have begun to identify quantitative trait nucleotides within several of the candidate genes (Lai *et al.* 1994; Long *et al.* 1998). The results reported here establish wing shape as another trait with great potential for understanding the molecular basis of morphological variation, given the advanced state of knowledge concerning wing patterning mechanisms.

Even without knowledge of the genes that correspond to QTL, our results provide several insights into the cell biology of variation in wing shape. First, they confirm that genetic effects on overall wing shape are likely to be mediated through local effects on wing shape, including the placement of wing veins. The genetic dissociation between wing size and wing shape supports the contention that regulation of cell size and number (McCabe *et al.* 1997) is only one mechanism by which wing shape may be controlled. Although Weber (1992) has clearly demonstrated that genetic variation for cell density in small patches of the wing blade exists, the independence of wing shape from the effects of sex and growth temperature, both of which greatly affect wing size, suggests that shape may be more directly regulated than size.

The possibility that the EGF pathway is a major source of variation for the shapes of intervein regions is consistent with our recent proposal that the wing veins are important determinants of wing shape (Birdsall *et al.* 2000). By regulating the amount of vein material that differentiates, this pathway may directly affect the length of each longitudinal vein. During and after metamorphosis, the tensile properties of veins would allow them to perform the role of a scaffold, or of drawstrings, that pulls the intervein regions into shape (Waddington 1940). On this view, cell density, at a quantitative level, is established as a secondary response to vein length. This does not preclude the regulation of cell growth and cell division, through genes such as *spalt* and *wingless*, from having an effect on wing shape, but it highlights the reality that mechanisms that act during cell division and pattern formation (including "entelechy"-like mechanisms; Garcia-Bellido and Garcia-Bellido 1998) are only one aspect of the regulation of wing shape.

Wing imaginal discs undergo waves of expansion during late third instar larvae and in pupae (Milan *et al.* 1996a,b), and the final distribution of cells is in large part a function of cell migration and differentiation (Gonzalez-Gaitan *et al.* 1994). It is thus not obvious that genes involved in pattern formation should be the major contributors to quantitative variation for wing shape. Despite their proximity to known genes, many of the QTL that we have identified could actually be as yet uncharacterized genes, with roles in processes such as local cell growth, cytoplasmic reorganization, cuticle secretion, and metabolic processes. For statistical reasons, the resolution of QTL analysis is not great enough to support positional cloning of candidate genes (Darvasi *et al.* 1993; Boehnke 1994). Consequently, the confirmation that a particular gene is in fact a candidate gene requires corroboration using independent genetic strategies such as quantitative complementation testing (Long *et al.* 1996; Lyman and Mackay 1998; A. Palsson and G. Gibson, unpublished results) and allelic association studies (Long and Langley 1999). Application of these methods will provide a test of the proposition that molecular variation in candidate genes identified through mutational screens is truly responsible for phenotypic variation in Drosophila wings.

We thank Kelly Ratcliff and Kelli Birdsall for help with dissections and landmark capture; Kate Teeter and Sylvie van Helden for performing the preliminary analyses of wing shape; Rob Gasperini and Lynn Stam for help in establishing the ASO method; Trudy Mackay, Sergei Nuzhdin, and Elena Pasyukova for genotyping and providing the RI lines; and Jeff Leips for the RI line genetic map. This work was supported by a fellowship from the David and Lucille Packard Foundation to G.G.

LITERATURE CITED

Basten, C. J., B. S. Weir and Z-B. Zeng, 1999 *QTL Cartographer Windows, Version 1.01*.

Birdsall, K., E. Zimmerman, K. Teeter and G. Gibson, 2000 Genetic variation for the positioning of wing veins in *Drosophila melanogaster*. Evol. Dev. **2:** 16–24.

Boehnke, M., 1994 Limits of resolution of genetic linkage studies: implications for the positional cloning of human disease genes. Am. J. Hum. Genet. **55:** 379–390.

Bookstein, F. L., 1991 *Morphometric Tools for Landmark Data: Geometry and Biology*. Cambridge University Press, New York.

Bookstein, F. L., 1994 Combining the tools of geometric morphometrics in *Advances in Morphometrics* (NATO AIS Series A, Life Sciences, Vol. 284), edited by L. Marcus, M. Corti, A. Loy, G. Naylor and D. Slice. Plenum, New York.

Darvasi, A., A. Weinreb, V. Minke, J. I. Weller and M. Soller, 1993 Detecting marker-QTL linkage and estimating QTL gene effect and map location using a saturated genetic map. Genetics **134:** 943–951.

de Celis, J. F., 1998 Positioning and differentiation of veins in the *Drosophila* wing. Int. J. Dev. Biol. **42:** 335–343.

de Moed, G. H., G. de Jong and W. Scharloo, 1997 The phenotypic plasticity of wing size in *Drosophila melanogaster*: the cellular basis of its genetic variation. Heredity **79:** 260–267.

Dryden, I. L., and K. V. Madia, 1998 *Statistical Shape Analysis*. Wiley-Interscience, New York.

Freeman, M., 1998 Complexity of EGF receptor signalling revealed in *Drosophila*. Curr. Opin. Genet. Dev. **8:** 407–411.

Garcia-Bellido, A. C., and A. Garcia-Bellido, 1998 Cell proliferation in the attainment of constant sizes and shapes: the Entelechia model. Int. J. Dev. Biol. **42:** 353–362.

Gibson, G., and S. van Helden, 1997 Is function of the Drosophila homeotic gene *Ultrabithorax* canalized? Genetics **147:** 1155–1168.
Gonzalez-Gaitan, M., M. P. Capdevila and A. Garcia-Bellido, 1994 Cell proliferation patterns in the wing imaginal disc of *Drosophila*. Mech. Dev. **46:** 183–200.
Gotzes, F., S. Balfanz and A. Baumann, 1994 Primary structure and functional characterization of a Drosophila dopamine receptor with high homology to human D1/5 receptors. Receptors Channels **2:** 131–141.
Guerra, D., M. C. Pezzoli, G. Giorgi, F. Garoia and S. Cavicchi, 1997 Developmental constraints in the *Drosophila* wing. Heredity **79:** 564–571.
Guichard, A., B. Biehs, M. A. Sturtevant, L. Wickline, J. Chacko *et al.*, 1999 *rhomboid* and *star* interact synergistically to promote EGFR/MAPK signaling during Drosophila wing vein development. Development **126:** 2663–2676.
James, A. C., R. B. Azevedo and L. Partridge, 1997 Genetic and environmental responses to temperature of *Drosophila melanogaster* from a latitudinal cline. Genetics **146:** 881–890.
Kacser, H., and J. A. Burns, 1981 The molecular basis of dominance. Genetics **97:** 639–666.
Keightley, P. D., K. Morris, A. Ishikawa, V. Falconer and F. Oliver, 1998 Test of candidate gene-quantitative trait locus association applied to fatness in mice. Heredity **81:** 630–637.
Lai, C., R. F. Lyman, A. D. Long, C. H. Langley and T. F. C. Mackay, 1994 Naturally occurring variation in bristle number and DNA polymorphisms at the *scabrous* locus of *Drosophila melanogaster*. Science **266:** 1697–1702.
Lander, E. S., and D. Botstein, 1989 Mapping Mendelian factors underlying quantitative traits using RFLP linkage maps. Genetics **121:** 185–199.
Liu, J., J. M. Mercer, L. Stam, G. Gibson, Z-B. Zeng *et al.*, 1996 Genetic analysis of a morphological shape difference in the male genitalia of *Drosophila simulans* and *D. mauritiana*. Genetics **142:** 1129–1145.
Long, A. D., and C. H. Langley, 1999 The power of association studies to detect the contribution of candidate genetic loci to variation in complex traits. Genome Res. **9:** 720–731.
Long, A. D., S. L. Mullaney, T. F. C. Mackay and C. H. Langley, 1996 Genetic interactions between naturally occurring alleles at quantitative trait loci and mutant alleles at candidate loci affecting bristle number in *Drosophila melanogaster*. Genetics **144:** 1497–1510.
Long, A. D., R. F. Lyman, C. H. Langley and T. F. C. Mackay, 1998 Two sites in the *Delta* gene region contribute to naturally occurring variation in bristle number in *Drosophila melanogaster*. Genetics **149:** 999–1017.
Lyman, R. F., and T. F. C. Mackay, 1998 Candidate quantitative trait loci and naturally occurring phenotypic variation for bristle number in *Drosophila melanogaster*: the *Delta-Hairless* gene region. Genetics **149:** 983–998.
Mackay, T. F. C., 1996 The nature of quantitative genetic variation revisited: lessons from *Drosophila* bristles. Bioessays **18:** 113–121.
Mayo, O., and R. Burger, 1997 The evolution of dominance: a theory whose time has passed? Biol. Rev. **72:** 97–110.
McCabe, J., V. French and L. Partridge, 1997 Joint regulation of cell size and cell number in the wing blade of *Drosophila melanogaster*. Genet. Res. **69:** 61–68.
Milan, M., S. Campuzano and A. Garcia-Bellido, 1996a Cell cycling and patterned cell proliferation in the wing primordium of *Drosophila*. Proc. Natl Acad. Sci. USA **93:** 640–645.
Milan, M., S. Campuzano and A. Garcia-Bellido, 1996b Cell cycling and patterned cell proliferation in the *Drosophila* wing during metamorphosis. Proc. Natl. Acad. Sci. USA **93:** 11687–11692.
Morata, G., and E. Sanchez-Herrero, 1999 Patterning mechanisms in the body trunk and the appendages of *Drosophila*. Development **126:** 2823–2828.
Nagaraj, R., A. T. Pickup, R. Howes, K. Moses, M. Freeman *et al.*, 1999 Role of the EGF receptor pathway in growth and patterning of the *Drosophila* wing through the regulation of *vestigial*. Development **126:** 975–985.
Nuzhdin, S. V., E. G. Pasyukova, C. L. Dilda, Z-B. Zeng and T. F. C. Mackay, 1997 Sex-specific quantitative trait loci affecting longevity in *Drosophila melanogaster*. Proc. Natl. Acad. Sci. USA **94:** 9734–9739.
Rasband, W., 1995 *NIH Image*. Springfield, VA.
Rohlf, F. J., 1993 Relative warp analysis and an example of its application to mosquito wings, pp. 131–159 in *Contributions to Morphometrics*, edited by L. F. Marcus, E. Bello and A. Garcia-Valedcasas. Museo Nacional de Ciencias Naturales, Valsain, Spain.
Saiki, R. K., T. L. Bugawan, G. T. Horn, K. B. Mullis and H. A. Erlich, 1986 Analysis of enzymatically amplified beta-globin and HLA-DQ alpha DNA with allele-specific oligonucleotide probes. Nature **324:** 163–166.
SAS Institute, 1990 *SAS/STAT User's Guide*. SAS Institute, Inc., Cary, NC.
SAS Institute, 1995 *JMP Introductory Guide*. SAS Institute, Inc., Cary, NC.
Sax, K., 1923 The association of size differences with seed-coat pattern and pigmentation in *Phaseolus vulgaris*. Genetics **8:** 522–560.
Schug, M. D., K. Wetterstrand, M. Gaudette, R. Lim, C. Hutter *et al.*, 1998 The distribution and frequency of microsatellite loci in *Drosophila melanogaster*. Mol. Ecol. **7:** 57–70.
Simcox, A., 1997 Differential requirement for EGF-like ligands in *Drosophila* wing development. Mech. Dev. **62:** 41–50.
Simon, M. A., G. S. Dodson and G. M. Rubin, 1993 An SH3-SH2-SH3 protein is required for p21Ras1 activation and binds to Sevenless and Sos proteins in vitro. Cell **73:** 169–177.
Strigini, M., and S. M. Cohen, 1999 Formation of morphogen gradients in the *Drosophila* wing. Semin. Cell. Dev. Biol. **10:** 335–344.
Teeter, K., M. Naeemuddin, R. Gasperni, E. Zimmerman, K. White *et al.*, 2000 Haplotype di-morphism in a SNP collection from *Drosophila melanogaster*. J. Exp. Zool. **288:** 63–75.
Waddington, C. H., 1940 The genetic control of wing development in *Drosophila*. Genetics **25:** 75–139.
Weber, K., 1992 How small are the smallest selectable domains of form? Genetics **130:** 345–353.
Weber, K., R. Eisman, L. Morey, A. Patty, J. Sparks *et al.*, 1999 An analysis of polygenes affecting wing shape on chromosome 3 in *Drosophila melanogaster*. Genetics **153:** 773–786.
Zeng, Z-B., 1993 Theoretical basis for separation of multiple linked gene effects in mapping quantitative trait loci. Proc. Natl. Acad. Sci. USA **90:** 10972–10976.
Zeng, Z-B., 1994 Precision mapping of quantitative trait loci. Genetics **136:** 1457–1468.

Communicating editor: L. Partridge